Hierarchical Liouville-Space Approach for Accurate and Universal Characterization of Quantum Impurity Systems

ZhenHua Li, NingHua Tong, Xiao Zheng, Dong Hou, JianHua Wei, Jie Hu, and YiJing Yan

Phys. Rev. Lett. **109**, 266403 — Published 26 December 2012

DOI: 10.1103/PhysRevLett.109.266403

Hierarchical Liouville-space approach for accurate and universal characterization of quantum impurity systems

ZhenHua Li,[1] NingHua Tong,[1] Xiao Zheng,[2,*] Dong Hou,[2]
JianHua Wei,[1,†] Jie Hu,[3,4] and YiJing Yan[2,3,‡]

[1]*Department of Physics, Renmin University of China, Beijing 100872, China*
[2]*Hefei National Laboratory for Physical Sciences at the Microscale, University of Science and Technology of China, Hefei, Anhui 230026, China*
[3]*Department of Chemistry, Hong Kong University of Science and Technology, Hong Kong, China*
[4]*Department of Physics, Capital Normal University, Beijing 100048, China*

(Dated: Submitted on June 18, 2012; revised on November 23, 2012)

Abstract

A hierarchical equations of motion (HEOM) based numerical approach is developed for accurate and efficient evaluation of dynamical observables of strongly correlated quantum impurity systems. This approach is capable of describing quantitatively Kondo resonance and Fermi liquid characteristics, achieving the accuracy of latest high-level numerical renormalization group approach, as demonstrated on single-impurity Anderson model systems. Its application to a two-impurity Anderson model results in differential conductance versus external bias, which correctly reproduces the continuous transition from Kondo states of individual impurity to singlet spin-states formed between two impurities. The outstanding performance on characterizing both equilibrium and nonequilibrium properties of quantum impurity systems makes the HEOM approach potentially useful for addressing strongly correlated lattice systems in the framework of dynamical mean field theory.

PACS numbers: 71.27.+a, 72.15.Qm

*Electronic address: xz58@ustc.edu.cn
†Electronic address: wjh@ruc.edu.cn
‡Electronic address: yyan@ust.hk

Quantum impurity systems cover a broad range of important physical systems where strong electron-electron (e-e) interactions among a few localized impurities affect crucially the system properties. Besides the e-e interactions, the impurities are coupled to the itinerant electrons in surrounding bulk materials, which serve as the electron reservoir and thermal bath. Moreover, some extensive strongly correlated systems can be treated as quantum impurity systems. For instance, the celebrated Hubbard model can be mapped onto an Anderson impurity system via a self-consistent dynamical mean-field theory [1]. The strong e-e interactions give rise to a variety of intriguing phenomena of prominent many-body nature, such as Kondo effects, Mott metal-insulator transition, and high-temperature superconductivity. Examples of localized impurities are the d- or f-electrons of transition metal atoms and electrons trapped in quantum dots.

Accurate characterization of quantum impurity systems is the key to the understanding of the mechanisms and effects of strong electron correlations. This has remained a very challenging task, especially for the quantitative evaluation of dynamical quantities directly related to experimental measurements, such as the projected density of states and spectral function of the localized impurities. A vast amount of theoretical efforts have been devoted to achieving this goal, including the quantum Monte Carlo (QMC) approach [2, 3], density matrix renormalization group method [4, 5], numerical renormalization group (NRG) method [6, 7], many-body perturbation theory [8], effective/quasi single-particle approaches [9, 10], *etc.* Despite their success in elucidating some fundamental features of electron correlations, the practicality of existing approaches has been limited within a few basic models [11–13]. The reason is mainly twofold: (*i*) the applicability of involving techniques relies critically on the system configuration, and (*ii*) the complexity of numerical algorithms increases dramatically with the number of impurities. Consequently, generalization of existing approaches [2–7] to more complex models is often difficult. Therefore, an accurate and universal approach capable of addressing strong correlation effects in general quantum impurity systems is highly desirable.

In this Letter we propose a general approach based on a hierarchical equations of motion (HEOM) formalism [14] to characterize quantum impurity systems from the perspective of open dissipative dynamics. The localized impurities constitute the open system of primary interest, while the surrounding reservoirs of itinerant electrons are treated as environment. The total Hamiltonian consists of the interacting impurities ($H_{\rm sys}$), the noninteracting elec-

tron reservoirs ($H_{\rm res}$), and their couplings $H_{\rm sys\text{-}res}=\sum_{\alpha\mu k}(t_{\alpha\mu k}\,\hat{a}^\dagger_\mu\hat{d}_{\alpha k}+{\rm H.c.})$. Here, $\hat{a}^\dagger_\mu$ and $\hat{a}_\mu$ denote the creation and annihilation operators for impurity state $|\mu\rangle$ (including spin, space, *etc.*), while $\hat{d}^\dagger_{\alpha k}$ and $\hat{d}_{\alpha k}$ are those for the α-reservoir state $|k\rangle$ of energy $\epsilon_{\alpha k}$. The influence of electron reservoirs on the impurities is taken into account through the hybridization functions, $\Delta_{\mu\nu}(\omega)\equiv\sum_\alpha\Delta_{\alpha\mu\nu}(\omega)=\pi\sum_{\alpha k}t_{\alpha\mu k}t^*_{\alpha\nu k}\,\delta(\omega-\epsilon_{\alpha k})$, in the absence of applied chemical potentials.

The HEOM that governs the dynamics of open system assumes the form of [14]:

$$\begin{aligned}\dot{\rho}^{(n)}_{j_1\cdots j_n}=&-\Big(i\mathcal{L}+\sum_{r=1}^{n}\gamma_{j_r}\Big)\rho^{(n)}_{j_1\cdots j_n}-i\sum_j\mathcal{A}_{\bar{j}}\,\rho^{(n+1)}_{j_1\cdots j_nj}\\&-i\sum_{r=1}^{n}(-)^{n-r}\,\mathcal{C}_{j_r}\,\rho^{(n-1)}_{j_1\cdots j_{r-1}j_{r+1}\cdots j_n}.\end{aligned}\tag{1}$$

The basic variables are the reduced system density operator $\rho^{(0)}(t)\equiv{\rm tr}_{\rm res}\,\rho_{\rm total}(t)$ and auxiliary density operators, $\{\rho^{(n)}_{j_1\cdots j_n}(t);n=1,\cdots,L\}$, with L denoting the terminal or truncated tier level. The Liouvillian of impurities, $\mathcal{L}\cdot\equiv\hbar^{-1}[H_{\rm sys},\cdot\,]$, may contain both e-e interaction and time-dependent external fields. The superoperators $\mathcal{A}_{\bar{j}}$ and $\mathcal{C}_j$ are expressed by Eq. (S1) of Ref. [15]. The index $j\equiv(\sigma\mu m)$ corresponds to the transfer of an electron to/from ($\sigma=+/-$) the impurity state μ, associated with the characteristic memory time γ_m^{-1}. The total number of distinct j-indexes involved is determined by the preset level of accuracy for decomposing reservoir correlation functions by exponential functions. Such a number draws the maximum tier level $L_{\rm max}$, at which Eq. (1) ultimately terminate [15]. The hierarchy is self-contained at $L=2$ for noninteracting $H_{\rm sys}$ [14]; while for $H_{\rm sys}$ involving e-e interactions, the solution of Eq. (1) must go through systematic tests to confirm its convergence versus L. In practice, a relatively low L (≈ 4) is usually sufficient to yield quantitatively converged results for weak and medium impurity-reservoir couplings.

The details of the HEOM formalism are referred to Refs. [14–17]. Here, we focus on some of its key features: (*i*) It is based on the Feynmann–Vernon path integral formalism [18], with fermionic operators represented by Grassmann variables [19]. (*ii*) It resolves nonperturbatively the combined effects of impurity-reservoir dissipation, e-e interactions, and non-Markovian memory [14]. (*iii*) The influence of reservoir environment on physical properties of impurities is taken into account via the hybridization functions, which enter Eq. (1) through a recently developed optimal Padé spectrum decomposition scheme [20, 21]. (*iv*) Besides the equilibrium dynamical observables, it is also capable of addressing

nonequilibrium response of quantum impurity systems to external fields such as laser pulses or applied voltages [17].

The HEOM approach has been applied to study static and transient electron transport through quantum dot systems, with which some interesting phenomena have been revealed, such as the dynamical Coulomb blockade [22] and dynamical Kondo transition [16].

In the framework of HEOM, there are two schemes to evaluate the dynamical observables of quantum impurity systems. (*i*) Calculate relevant system correlation/response functions based on an HEOM-space linear response theory [15]. The correlation function for two arbitrary system operators $\hat{A}$ and $\hat{B}$ is $\widetilde{C}_{AB}(t) \equiv \langle \hat{A}(t)\hat{B}(0)\rangle = \mathrm{tr}_{\mathrm{total}}[\hat{A}(t)\hat{B}(0)\rho^{\mathrm{eq}}_{\mathrm{total}}(T)]$, where $\rho^{\mathrm{eq}}_{\mathrm{total}}(T)$ is the equilibrium density operator of the total system. $\widetilde{C}_{AB}(t)$ can be evaluated by using the quantum Liouville propagator in the HEOM space [15]. Let $C_{AB}(\omega) \equiv \frac{1}{2}\int dt\, e^{i\omega t}\widetilde{C}_{AB}(t)$, which satisfies the detailed balance relation of $C_{BA}(-\omega) = e^{-\omega/k_BT}C_{AB}(\omega)$. The corresponding spectral function is $J_{AB}(\omega) \equiv \frac{1}{2\pi}\int dt\, e^{i\omega t}\langle\{\hat{A}(t),\hat{B}(0)\}\rangle = \frac{1}{\pi}\left(1+e^{-\omega/k_BT}\right)C_{AB}(\omega)$. In particular, with $\hat{A} = \hat{B}^\dagger = \hat{a}_\mu$, $J_{\hat{a}_\mu\hat{a}^\dagger_\mu}(\omega) = A_\mu(\omega)$ gives the spectral density of impurity state μ, which can be measured experimentally via angle-resolved photoemission spectroscopy [23] and scanning tunneling microscope [24]. (*ii*) Solve Eq. (1) for nonequilibrium electronic response under external perturbation. For instance, the differential conductance (dI/dV) can be calculated via the response current under applied bias, followed by a finite difference analysis. The above two schemes are completely equivalent for linear response properties.

It is emphasized that the HEOM approach is distinctly different from the conventional equations of motion (EOM) method using many-body Green's functions (GFs) as basic variables [25]. The GF–EOM method often treats the impurities and reservoirs on equal footing. To close the equations it invokes specific approximations for individual GFs. In contrast, the HEOM approach focuses on the impurities, with all reservoir degrees of freedom averaged out properly [14]. Consequently, the HEOM involve much fewer unknowns than GF–EOM at same tier level. Moreover, the generic form of Eq. (1) applies to any complex impurity system, without additional derivation effort. Therefore, the HEOM approach outperforms GF–EOM in terms of both efficiency and universality [15].

For numerical demonstrations, consider first an asymmetric single-impurity Anderson model (SIAM) system that has been widely studied [26]. $H_{\mathrm{sys}} = \epsilon_{\mathrm{d}}(\hat{n}_\uparrow + \hat{n}_\downarrow) + U\hat{n}_\uparrow\hat{n}_\downarrow$, where $\hat{n}_\mu = \hat{a}^\dagger_\mu\hat{a}_\mu$ and $U \neq -2\,\epsilon_{\mathrm{d}}$. Lorentzian hybridization functions, $\Delta_{\mu\nu}(\omega) = \delta_{\mu\nu}\Delta W^2/(\omega^2 +$

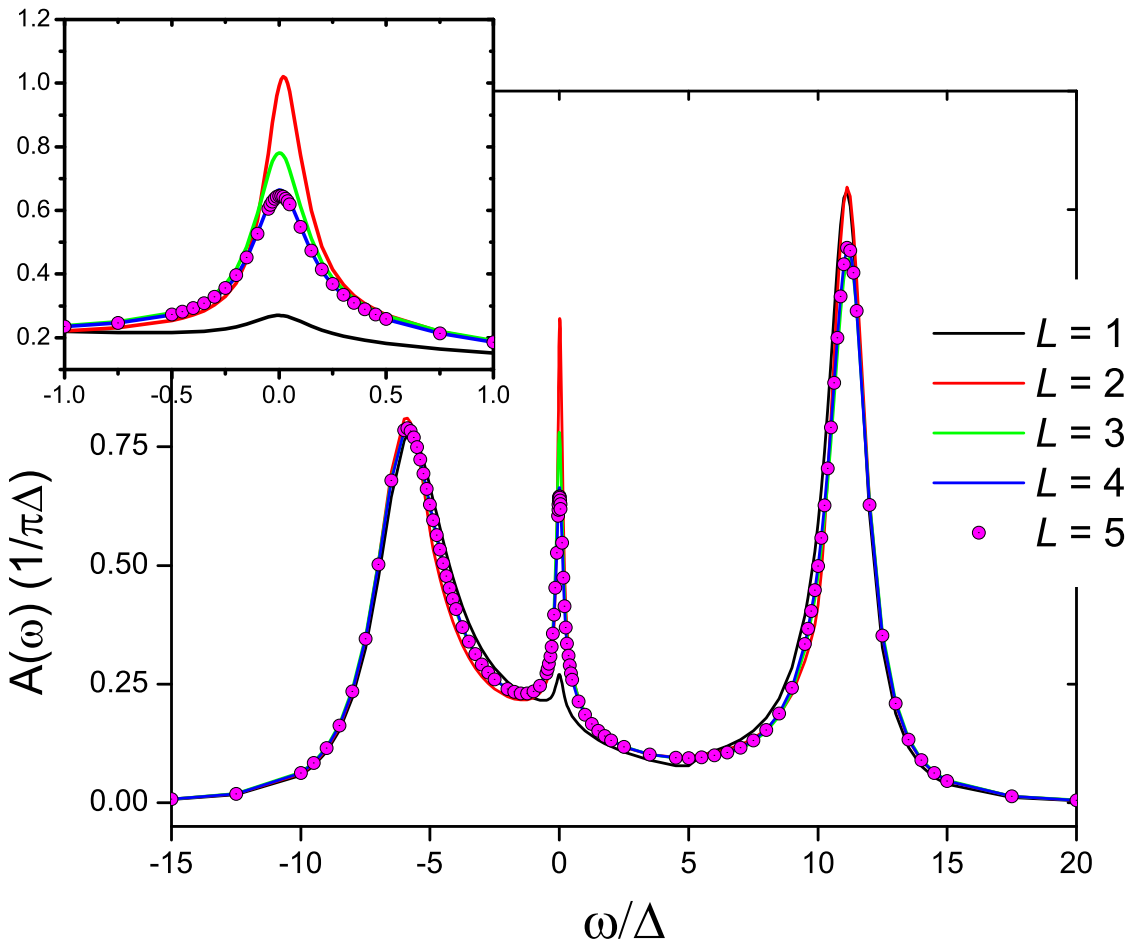

FIG. 1: (Color online). The spin-up or down spectral function of an asymmetric SIAM calculated by the HEOM approach at different truncation tiers. The inset magnifies the Kondo resonance peak at $\omega = 0$. The parameters adopted are $\epsilon_{\rm d} = -5$, $U = 15$, $W = 10$, and $T = 0.075$ (in unit of Δ).

W^2), are adopted, with Δ being the effective impurity-reservoir coupling strength and W the reservoir band width. Figure 1 depicts the calculated impurity spectral function $A(\omega)$ by the HEOM approach, up to the converged tier level. The well-known spectral features of SIAM are clearly resolved: (*i*) The two resonance peaks at around $\omega = \epsilon_{\rm d}$ and $U + \epsilon_{\rm d}$ correspond to the excitation energies associated with change of impurity occupancy state. (*ii*) The peak at the Fermi energy ($\omega = E_F \equiv 0$) highlights the presence of Kondo resonance under a low temperature. (*iii*) The sum rule $\int A(\omega)\, d\omega = 1$ is satisfied to numerical precision. The comparison in Fig. 1 demonstrates distinctly that the HEOM results converge rapidly with L for full energy range. This confirms that the HEOM results converge quantitatively at a

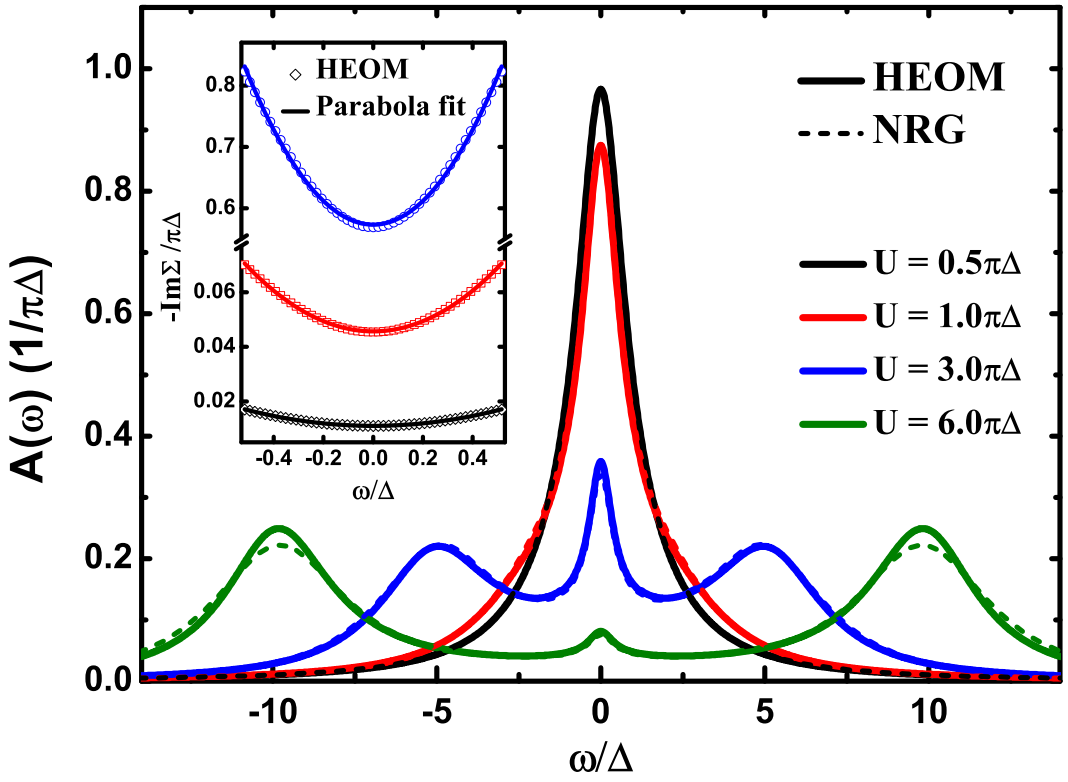

FIG. 2: (Color online). Comparison between $A(\omega)$ of symmetric SIAM calculated by HEOM and NRG methods. The parameters adopted are $T = 0.2$ and $W = 50$ (in unit of Δ). The inset shows the imaginary part of interaction self-energy calculated from HEOM at energy close to $\omega = 0$.

relatively low truncation level, even in the Kondo regime.

Figure 2 depicts the calculated $A(\omega)$ of a symmetric ($U = -2\epsilon_{\rm d}$) SIAM, from weak ($U = 0.5\pi\Delta$) to strong ($U = 6\pi\Delta$) e-e interactions. For comparison, we also show results obtained by using the full density matrix NRG method [27], where a self-energy scheme of Ref. [28] is employed, and the results are averaged over 8 different logarithmic discretizations [29]. Note that our NRG data in Fig. 2 differ slightly from those in Ref. [30], due to different $\Delta_{\mu\nu}(\omega)$ used (Lorentzian versus constant). Apparently, the two sets of curves agree quantitatively at all values of U studied. In the weak ($U = 0.5$ and $1.0\,\pi\Delta$) and intermediate ($U = 3\pi\Delta$) interaction regimes, HEOM and NRG curves almost overlap with each other; while in the strong ($U = 6\pi\Delta$) interaction regime minor deviation is observed in the height of Hubbard peaks, which is possibly due to remaining uncertainty in NRG results [15]. Therefore, such a benchmark comparison clearly affirms that the HEOM approach achieves the same level of accuracy as the latest high-level NRG method.

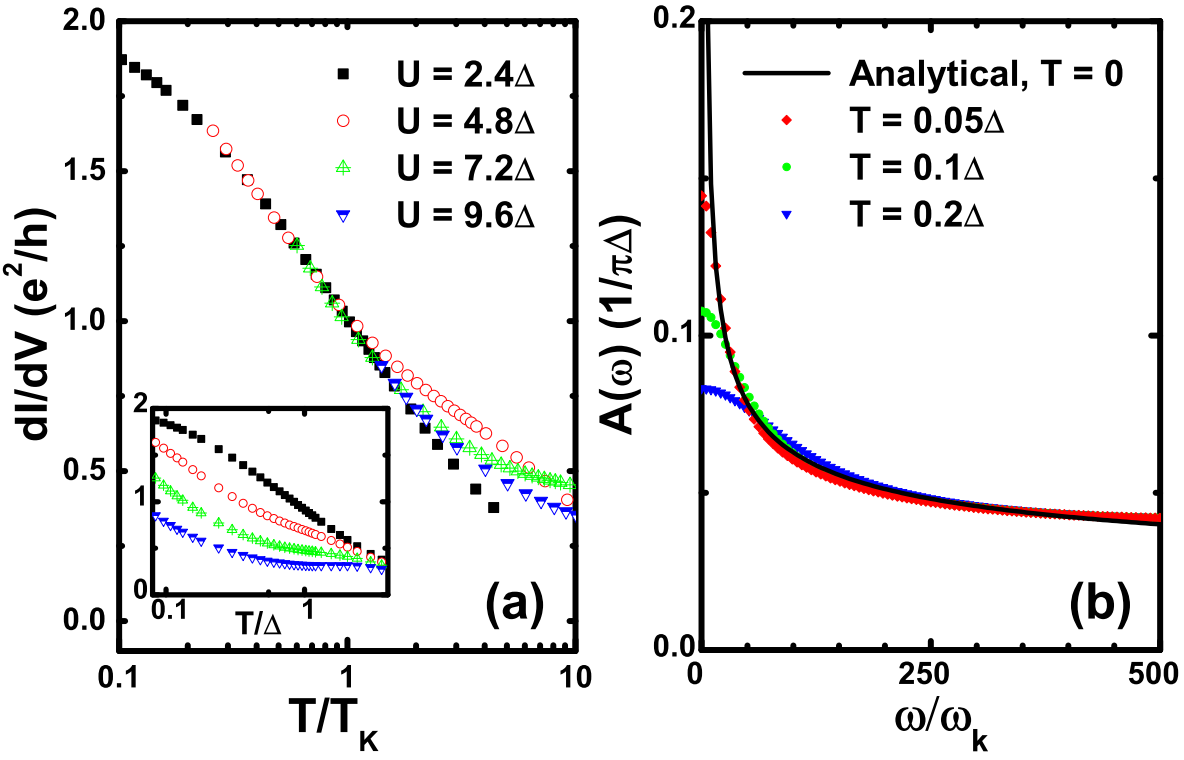

FIG. 3: (Color online). (a) dI/dV versus T/T_K for symmetric SIAM with $T_K = (U\Delta/2)^{\frac{1}{2}}\, e^{-\pi U/8\Delta+\pi\Delta/2U}$ [26] and $W = 24\Delta$. The inset depicts dI/dV versus unscaled T. (b) Comparison between the HEOM numerical results and an analytical expression, Eq. (4.2) of Ref. [35], for the large–ω tail of $A(\omega)$. Other parameters adopted are (in unit of Δ): $W = 100$, $U = -2\epsilon_{\rm d} = 6\pi$. See Ref. [15] for more details.

Highlighted in the inset of Fig. 2 are the imaginary part of interaction self-energy (circles), exhibiting a parabolic lineshape near $\omega = E_F \equiv 0$ (lines). This is a clear indication of Fermi liquid character [26]. Luttinger has proved that the Kondo peak height is exactly $1/\pi\Delta$ for a symmetric SIAM at $T = 0$, independent of U [31]. At finite T and U, it is expected that in general $A(\omega = 0) < 1/\pi\Delta$ [32], as exemplified by both Fig. 1 and Fig. 2.

The HEOM results exhibit the correct scaling behavior by Kondo temperature T_K [33, 34]. This is verified by the calculated dI/dV versus T/T_K as depicted in Fig. 3(a), where the universal scaling is clearly manifested at $T < T_K$ and $\Delta \ll U \ll W$. Moreover, as T is lowered, the calculated $A(\omega)$ draws progressively to an analytic curve of a logarithmic form predicted in Ref. [35]; see Fig. 3(b).

We also compare HEOM with the latest continuous time QMC (CTQMC) approach [3] on

the SIAM studied in Fig. 2. Both approaches yield quantitatively consistent imaginary time GFs with a maximum relative deviation less than 5%. However, $A(\omega)$ of CTQMC suffer from nontrivial uncertainties in analytical continuation of GFs to real energies by the maximum entropy method [15]. We then extend the comparison to the exact diagonalization [36–38], the slave-boson mean-field theory [39], and the non-crossing approximation [40]. The HEOM approach is apparently much more accurate than these methods [15]. In contrast to the fact that some existing methods would encounter practical or intrinsic problems in treating certain forms of e-e interactions, the HEOM approach admits an arbitrary form of e-e interaction (including spin-flip, electron-pair hopping, and nonlocal Coulomb interaction [41]) without additional computational cost, as long as it works with the full impurities Fock space.

The computational cost (time and memory) of present HEOM approach grows rapidly with the lowered T. This is because the resolution of long-time memory requires more exponential functions, and a higher L is usually necessary to achieve quantitative convergence. In particular, the cost for producing $A(\omega)$ of Fig. 2 is comparable to that required for NRG and CTQMC [15]; while at a higher T, the HEOM approach would be orders of magnitude faster. Whereas at extremely low T or large Δ, the present HEOM approach may be very expensive. It is however possible to reduce the computational cost significantly by designing more efficient reservoir memory decomposition schemes.

We proceed to demonstrate that the applicability of HEOM approach can be extended beyond the simple SIAM model and equilibrium properties. To this end, a parallel-coupled two-impurity Anderson model (TIAM) sketched in Fig. 4(a) is considered, where $H_{\rm sys} = H_1 + H_2 + V_{12}$, with H_1 (H_2) being the SIAM Hamiltonian for the impurity 1 (2), and $V_{12} = t(\hat{a}^\dagger_{1\uparrow}\hat{a}_{2\uparrow} + \hat{a}^\dagger_{1\downarrow}\hat{a}_{2\downarrow} + \text{H.c.})$. Such a TIAM model has been realized experimentally via a double quantum dot system, with the inter-dot coupling strength t tuned by plunger gates [42]. The nonzero t gives rise to an effective anti-ferromagnetic coupling, $J = 4t^2/U$, between the local spin moments at the two impurities. At a weak J, the two spin moments are nearly independent of each other, and the local spin at each impurity is screened by itinerant electrons separately. In contrast, at a sufficiently strong J, singlet spin-states covering both impurities are formed. Therefore, by varying the strength of t, the TIAM undergoes a continuous transition from Kondo singlet states of individual impurity to singlet spin-states formed between two impurities, as confirmed by NRG and conformal-field-theory

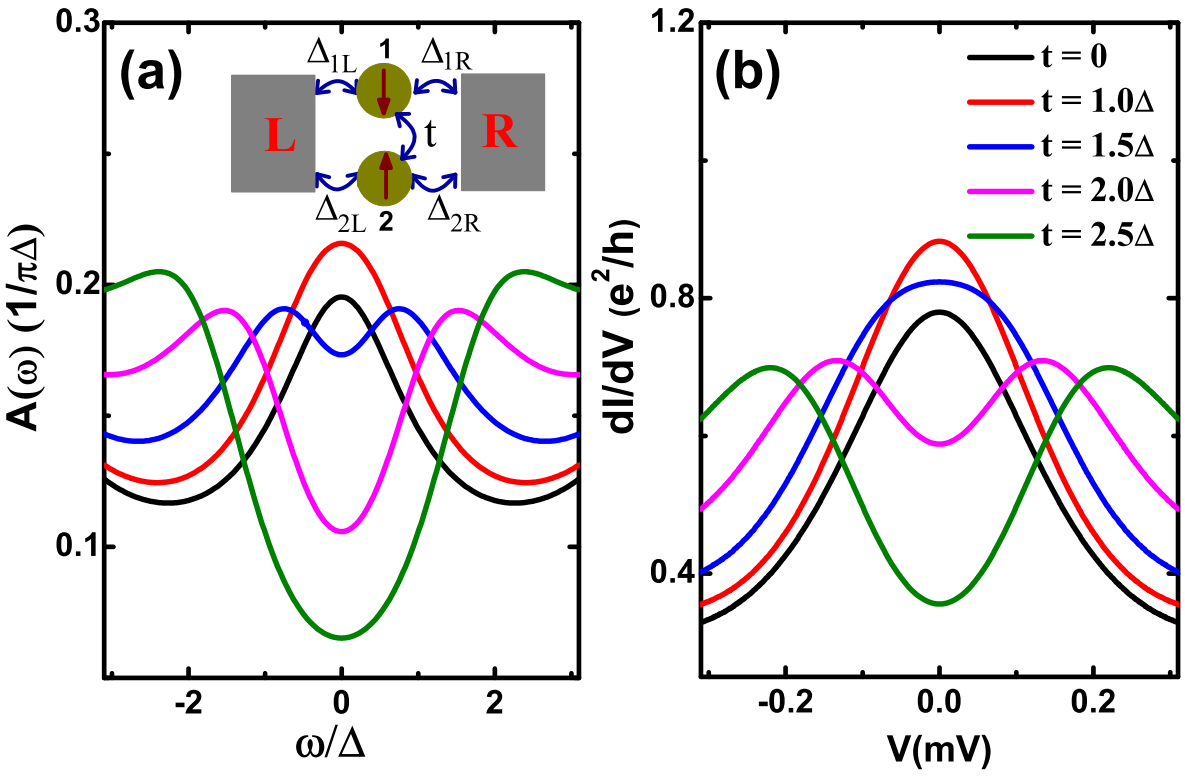

FIG. 4: (Color online). (a) $A(\omega)$ and (b) dI/dV versus V of a TIAM at various inter-impurity coupling strength ranging from 0 to 2.5Δ. The TIAM system is sketched in (a). The parameters adopted are (in unit of Δ): $W = 10$, $U_1 = U_2 = 10$, $\epsilon_1 = \epsilon_2 = -5$, and $T = 0.5$.

calculations [43, 44].

The HEOM approach is applied to evaluate the equilibrium spectral function $A(\omega)$ of a TIAM consisting of two identical impurities, along with its dI/dV versus external bias V. The latter is a nonequilibrium property, and is achieved via a finite difference approach [15]. The response current is extracted from first-tier ($n = 1$) auxiliary density operators [14]. Figure 4(a) and (b) depict the calculated $A(\omega) \equiv A_1(\omega) = A_2(\omega)$ and $dI/dV - V$, respectively. Apparently, the variation of $A(\omega)$ and $dI/dV - V$ with increasing t are analogous to each other. Their common features are as follows. (i) The system undergoes a transition from a Kondo singlet involving individual impurity (characterized by the single-peaked lineshape) at $t < \Delta$, to the singlet spin-state between two impurities (characterized by the double-peaked lineshape) at $t > 1.5\,\Delta$. (ii) The transition exhibits continuous crossover. As t increases, the single Kondo peak first broadens and approaches to its maximal height before it drops and splits into two. These features are consistent with previous experimental

[42] and theoretical [43, 44] investigations.

To summarize, the practicality of our developed hierarchical Liouville-space approach is demonstrated through studies on Anderson impurity models, where the key Kondo resonance and Fermi liquid features due to strong e-e interaction are accurately characterized. The HEOM approach can be straightforwardly extended to more complex quantum impurity models (such as multi-impurity models) without additional derivation and programming efforts [15]. Once converged, the HEOM results can serve as benchmarks to calibrate approximate numerical approaches, particularly the effective single-electron approaches, which are useful for studying more complex systems. Moreover, it is anticipated that HEOM would become a promising impurity solver for characterizing strongly correlated lattice systems in the framework of dynamical mean field theory [1].

The support from the Hong Kong UGC (AoE/P-04/08-2)(YJY), the NSF of China (Nos. 11074302, 11074303, 21103157, 21033008, 21233007), the Fundamental Research Funds for Central Universities of China (Nos. 2340000034, 2340000025)(XZ), the Research Funds of Renmin University of China (No. 11XNJ026)(JHW), and the China NKBRFSC (No. 2012CB921704)(NHT) is gratefully appreciated. We thank P. Werner, W. Wu, L. Huang, L. Du, and X. Dai for their help on CTQMC calculations.

---

[1] A. Georges, G. Kotliar, W. Krauth, and M. J. Rozenberg, Rev. Mod. Phys. **68**, 13 (1996).

[2] J. E. Hirsch and R. M. Fye, Phys. Rev. Lett. **56**, 2521 (1986).

[3] E. Gull, et al., Rev. Mod. Phys. **83**, 349 (2011).

[4] S. R. White, Phys. Rev. Lett. **69**, 2863 (1992).

[5] G. Vidal, Phys. Rev. Lett. **91**, 147902 (2003).

[6] K. G. Wilson, Rev. Mod. Phys. **47**, 773 (1975).

[7] R. Bulla, T. A. Costi, and T. Pruschke, Rev. Mod. Phys. **80**, 395 (2008).

[8] E. Khosravi et al., Phys. Rev. B **85**, 075103 (2012).

[9] K. S. Thygesen and A. Rubio, Phys. Rev. B **77**, 115333 (2008).

[10] S. Kurth, G. Stefanucci, E. Khosravi, C. Verdozzi, and E. K. U. Gross, Phys. Rev. Lett. **104**, 236801 (2010).

[11] P. W. Anderson, Phys. Rev. **124**, 41 (1961).

[12] J. Hubbard, Proc. Roy. Soc. A **276**, 238 (1963).

[13] P. A. Lee, T. M. Rice, J. W. Serene, L. J. Sham, and J. W. Wilkins, Comments on Cond. Matter Phys. **12**, 99 (1986).

[14] J. S. Jin, X. Zheng, and Y. J. Yan, J. Chem. Phys. **128**, 234703 (2008).

[15] For details, see Supplemental Materials.

[16] X. Zheng, J. S. Jin, S. Welack, M. Luo, and Y. J. Yan, J. Chem. Phys. **130**, 164708 (2009).

[17] X. Zheng et al., Prog. Chem. **24**, 1129 (2012).

[18] R. P. Feynman and F. L. Vernon, Jr., Ann. Phys. **24**, 118 (1963).

[19] L. H. Ryder, *Quantum Field Theory*, 2nd ed., Cambridge University Press, Cambridge, 1996.

[20] J. Hu, R. X. Xu, and Y. J. Yan, J. Chem. Phys. **133**, 101106 (2010).

[21] J. Hu, M. Luo, F. Jiang, R. X. Xu, and Y. J. Yan, J. Chem. Phys. **134**, 244106 (2011).

[22] X. Zheng, J. S. Jin, and Y. J. Yan, New J. Phys. **10**, 093016 (2008).

[23] A. Damascelli, Z. Hussain, and Z. X. Shen, Rev. Mod. Phys. **75**, 473 (2003).

[24] O. Y. Kolesnychenko et al., Phys. Rev. B **72**, 085456 (2005).

[25] H.-G. Luo, J.-J. Ying, and S.-J. Wang, Phys. Rev. B **59**, 9710 (1999).

[26] A. C. Hewson, *The Kondo Problem to Heavy-Fermions*, Cambridge University Press, Cambridge, 1993.

[27] A. Weichselbaum and J. von Delft, Phys. Rev. Lett. **99**, 076402 (2007).

[28] R. Bulla, A. C. Hewson, and T. Pruschke, J. Phys.: Condens. Matter **10**, 8365 (1998).

[29] W. C. Oliveira and L. N. Oliveira, Phys. Rev. B **49**, 11986 (1994).

[30] A. Isidori, D. Roosen, L. Bartosch, W. Hofstetter, and P. Kopietz, Phys. Rev. B **81**, 235120 (2010).

[31] J. M. Luttinger, Phys. Rev. **121**, 942 (1961).

[32] K. Yamada, Prog. Theor. Phys. **53**, 970 (1975).

[33] H. R. Krishna-murthy, J. W. Wilkins, and K. G. Wilson, Phys. Rev. B **21**, 1003 (1980).

[34] H. R. Krishna-murthy, J. W. Wilkins, and K. G. Wilson, Phys. Rev. B **21**, 1044 (1980).

[35] N. L. Dickens and D. E. Logan, J. Phys.: Condens. Matter **13**, 4505 (2001).

[36] E. Dagotto, Rev. Mod. Phys. **66**, 763 (1994).

[37] M. Caffarel and W. Krauth, Phys. Rev. Lett. **72**, 1545 (1994).

[38] Q. Si, M. J. Rozenberg, G. Kotliar, and A. E. Ruckenstein, Phys. Rev. Lett. **72**, 2761 (1994).

[39] G. Kotliar and A. E. Ruckenstein, Phys. Rev. Lett. **57**, 1362 (1986).

[40] N. E. Bickers, Rev. Mod. Phys. **59**, 845 (1987).

[41] J. Hubbard, Proc. R. Soc. Lond. A **277**, 237 (1964).

[42] J. C. Chen, A. M. Chang, and M. R. Melloch, Phys. Rev. Lett. **92**, 176801 (2004).

[43] O. Sakai, Y. Shimizu, and T. Kasuya, Solid State Commun. **75**, 81 (1990).

[44] I. Affleck, A. W. W. Ludwig, and B. A. Jones, Phys. Rev. B **52**, 9528 (1995).